

SIMULATION OF SEPIC CONTROLLER FOR BRUSHLESS DC MOTOR DRIVE TO IMPROVE INPUT POWER FACTOR

M.V.Ramana Rao P.V.N.Prasad*

Assistant Professor and Research Scholar, Professor*, Department of Electrical Engg., University College of Engg.
Osmania University, Hyderabad, A.P. India.

Phone : 040-27098628, E-mail : ramanarao2@yahoo.co.in, polaki@rediffmail.com*

Abstract: This paper evaluates the simplified converter topology for driving a permanent magnet brushless dc (BLDC) motor and improve the power factor with unipolar inverter and SEPIC (Single Ended Primary Inductance Converter) controller. The SEPIC converter is designed to operate as a voltage follower, the line current follows the line voltage waveform to a certain extent which improves the input power factor. The reduction in low-order harmonics and improved power factor is achieved without the use of any additional circuitry. With the growing potential for widespread use of permanent magnet brushless dc motor (BLDC) drives in many low-cost applications. The simplicity and reduced parts count of the proposed topology make it an attractive low cost choice for BLDC motor drives.

Key words: BLDC, SEPIC controller, Unipolar converter

Nomenclature

V_a, V_b, V_c	Voltagess of phases A, B, C respectively
e_a, e_b, e_c	Phase back emfs (V)
E	Back emf (V)
i_a, i_b, i_c	Phase currents (A)
R	Resistance of each phase winding (Ω)
L_s	Self inductance of each phase winding (H)
M	Mutual inductance between the windings
T_e	Electromagnetic torque (N-m)
T	Output torque (N-m)
T_L	Load torque(N-m)
J	Moment of inertia of rotor (kg-m^2)
B	Viscous friction coefficient (Nm-s/rad)
θ	Angular position of the rotor (rad)
ω_r	Angular speed of the rotor (rad/s)
L	Inductance of stator phase winding (H)
p	No. of poles
B_k	k_{th} harmonic coefficient
N	Number of winding turns per phase
l	Length of the rotor
r	internal radius of the rotor
S_1	Switch
D_1	Diode
C_{in}	Input capacitor
$C1, C2$	Capacitors
V_{in}	Input voltage (V)
$L1, L2$	Inductors
k_e	back EMF constant in V-s/rad

$B_{ak} = B_{bk} = B_{ck} = B_k$: k_{th} harmonic coefficient

I_{D1} Diode current

V_{L1}, V_{L2} Voltage across L_1 and L_2

1. Introduction

Permanent magnet brushless dc (BLDC) motor drives are widely used high volume low cost applications. Such applications are to be found in HVAC, fans, pumps, washers, dryers, tread mills and other exercise equipment, wheel chairs, people carriers in airport lobbies, golf carts, freezers, refrigerators, automobiles, hand tools, and small-process drives with velocity control for packaging, bottling, and food processing applications and many others in the range of fractional to 1-hp rating. The growth in the market of Permanent magnet BLDC motor drives has demanded the need of simulation tools capable of handling motor drive simulations. Simulations have helped the process of developing new systems including motor drives, by reducing cost and time. Simulation tools have the capabilities of performing dynamic simulations of motor drives in a visual environment so as to facilitate the development of new systems.

Brushless DC (BLDC) motors also known as electronically commutated motors (ECMs, EC motors). BLDC motors advantages over brushed DC motors, including more torque per weight and efficiency, reliability, reduced noise, longer lifetime elimination of ionizing sparks from the commutator and overall reduction of electromagnetic interference (EMI). With no windings on the rotor, they are not subjected to centrifugal forces, and because the windings are supported by the housing, they can be cooled by conduction, requiring no airflow inside the motor for cooling. [1],[2],[3].

2. Mathematical analysis of BLDC

The equation of each armature winding can be represented as follows : [2], [3].

$$V_a = Ri_a + L \frac{di_a}{dt} + e_a \quad (1)$$

$$V_b = Ri_b + L \frac{di_b}{dt} + e_b \quad (2)$$

(3)

$$i_a = \frac{1}{L_s - M} \int (V_a - e_a - R i_a) \cdot dt \quad (4)$$

$$i_b = \frac{1}{L_b - M} \int (V_b - e_b - R i_b) \cdot dt \quad (5)$$

$$i_c = \frac{1}{L_s - M} \int (V_c - e_c - R i_c) \cdot dt \quad (6)$$

$$e_a = k_e \cdot \omega_r \cdot \sum_{k=1}^{\infty} B_{ak} \cdot \sin[k(\theta)] \quad (7)$$

$$e_b = k_e \cdot \omega_r \cdot \sum_{k=1}^{\infty} B_{bk} \cdot \sin \left[k \left(\theta - \frac{2\pi}{3} \right) \right] \quad (8)$$

$$e_c = k_e \cdot \omega_r \cdot \sum_{k=1}^{\infty} B_{ck} \cdot \sin \left[k \left(\theta - \frac{4\pi}{3} \right) \right] \quad (9)$$

$$T_e = \frac{e_a i_a + e_b i_b + e_c i_c}{\omega_r} \quad (10)$$
$$T_e = J \frac{d\omega_r}{dt} + B\omega_r + T_L \quad (11)$$
$$\varpi_r = \frac{1}{J} \int (T_e - T_L) \cdot dt \quad (12)$$
$$E = 2NlrB\omega \quad (13)$$

$$T = \frac{1}{2} i^2 \frac{dL}{d\theta} - \frac{1}{2} B^2 \frac{dR}{d\theta} + (2NBrli) \quad (14)$$

Single-ended primary-inductor converter (SEPIC) is a type of DC-DC converter that allows the electrical potential (voltage) at its output to be greater than, less than, or equal to that at its input; the output of the SEPIC is controlled by the duty cycle of the control transistor. A SEPIC is similar to a traditional buck-boost converter.

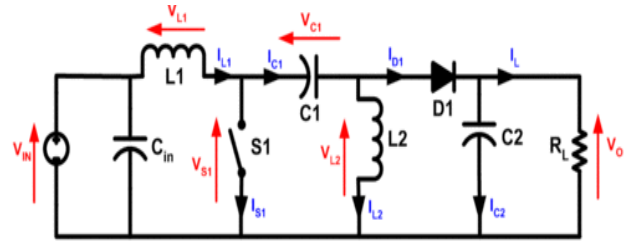


Fig. 1 Schematic of SEPIC Converter

The schematic diagram for a basic SEPIC is shown in Fig.1 Like other switched mode power supplies the SEPIC exchanges energy between the capacitors and inductors in order to convert from one voltage to another. The amount of energy exchanged is controlled by switch S1, which is typically a transistor such as a MOSFET. MOSFETs offer much higher input impedance and lower voltage drop than bipolar junction transistors (BJTs), and do not require biasing resistors as MOSFET switching is controlled by differences in voltage rather than a current, as with BJTs. [4]

4. Operation of SEPIC

A SEPIC is said to be in continuous-conduction mode if the current through the inductor L1 never falls to zero. During a SEPIC's steady-state operation, the average voltage across capacitor C1 (V_{C1}) is equal to the input voltage (V_{IN}). Because capacitor C1 blocks direct current, the average current across it (I_{C1}) is zero, making inductor L2 the only source of load current. Therefore, the average current through inductor L2 (I_{L2}) is the same as the average load current and hence independent of the input voltage.

Looking at average voltages, the following can be written:

$$V_{IN} = V_{L1} + V_{C1} + V_{L2} \quad (15)$$

Because the average voltage of V_{C1} is equal to V_{IN} , $V_{L1} = -V_{L2}$. For this reason, the two inductors can be wound on the same core. Since the voltages are the same in magnitude, their effects of the mutual inductance will be zero, since the voltages are the same in magnitude, the ripple currents from the two inductors will be equal in magnitude. [5]

The average currents can be summed as follows:

$$I_{D1} = I_{L1} - I_{L2} \quad (16)$$

When switch S1 is turned on, current I_{L1} increases and the current I_{L2} increases in the negative

direction. The energy to increase the current I_{L1} comes from the input source. Since S1 is a short while closed, and the instantaneous voltage V_{C1} is approximately V_{IN} , the voltage V_{L2} is approximately $-V_{IN}$. Therefore, the capacitor C1 supplies the energy to increase the magnitude of the current in I_{L2} and thus increase the energy stored in L2. The easiest way to visualize this is to consider the bias voltages of the circuit in a d.c. state, then close S1.

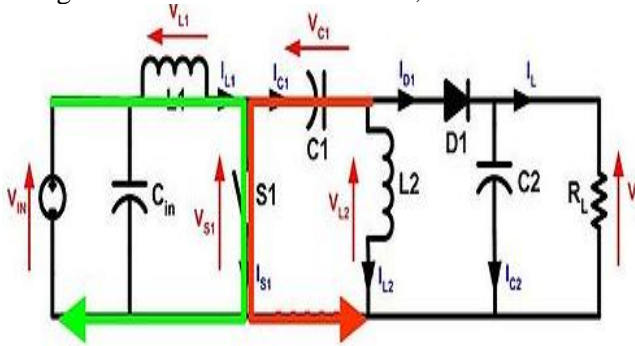


Fig. 2 With S1 closed current increases through L1 (green) and C1 discharges increasing current in L2 (red)

When switch S1 is turned off, the current I_{C1} becomes the same as the current I_{L1} , since inductors do not allow instantaneous changes in current. The current I_{L2} will continue in the negative direction, in fact it never reverses direction. It can be seen from the diagram that a negative I_{L2} will add to the current I_{L1} to increase the current delivered to the load. Using Kirchoff's Current Law, it can be shown that $I_{D1} = I_{C1} - I_{L2}$. It can then be concluded, that while S1 is off, power is delivered to the load from both L2 and L1. C1, however is being charged by L1 during

this off cycle, and will in turn recharge L2 during the on cycle. [6-9]

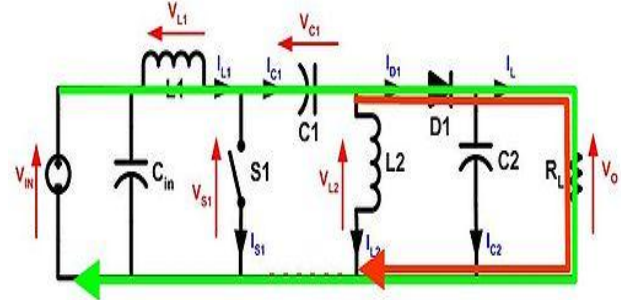


Fig. 3 With S1 open current through L1 (green) and current through L2 (red) produce current through the load.

5. Simulation of SEPIC controller for BLDC motor drive

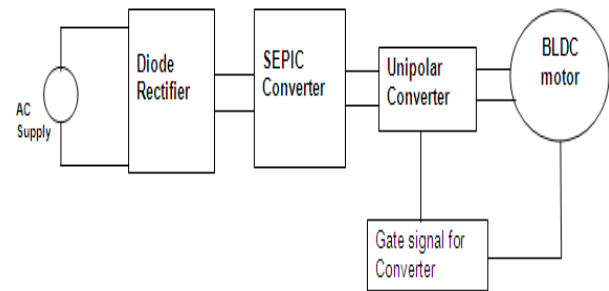


Fig. 4 Block Diagram of Unipolar BLDC motor Drive

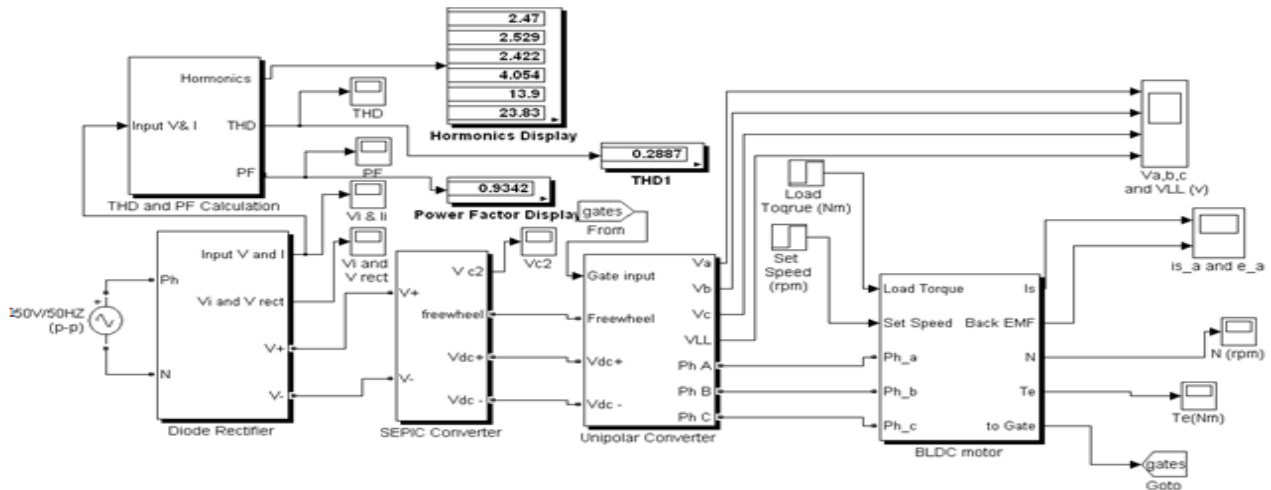


Fig. 5 Main simulink diagram of SEPIC converter BLDC motor

The Main block diagram of the unipolar converter for BLDC drive system is shown in Fig. 4. The Simulation diagram of SEPIC converter BLDC motor drive is as shown in fig.5. A voltage source of 50V, 50Hz AC supply connected to Drive. The AC

input is rectified using diode rectifier and converted into DC supply. This DC power is regulated using DC-DC converter which is Single Ended Primary Inductance converter (SEPIC) here. This DC-DC converter is used to improve the input power factor

of the AC supply and to minimize harmonics in the input current. Then the DC power is supplied to BLDC motor through unipolar power converter. The rotor position is sensed by hall sensors. The hall sensor signals and actual speed of BLDC motor are given to speed controller to generate gate signals for the unipolar converter in order to control the speed. The output of speed controller is connected to gates of the unipolar power converter. Based on switching of power converter devices, the BLDC motor stator winding is excited sequentially so as to develop electromagnetic torque in the motor to meet the load torque. The diode rectifier converts the AC input into uncontrolled DC. SEPIC controller is useful in input power factor improvement. This is implemented using simulink using MOSFET and other circuitry. The gate of MOSFET driven by the SEPIC Gate controller which uses of PI controller. [10 - 13].

6. Simulation results

The speed of the BLDC motor has set to a value of 1000 rpm reference speed or set speed and a constant load torque of 5 N.m applied to the motor at 0.04 sec. The corresponding speed response curve is as shown in Fig 6. The electromagnetic torque (T_e) developed by BLDC motor and the load torque is as shown in Fig. 7.

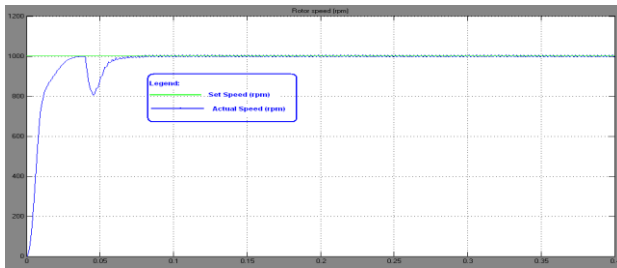


Fig.6 Rotor Speed Curve at 1000 rpm

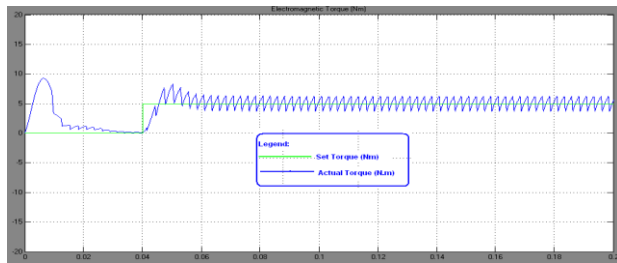


Fig. 7 Torque Curve at 1000 rpm

The input current found almost following the input voltage and maintained the power factor above 0.94 as shown in Fig. 8. As the current is periodic waveform the even harmonic components will be zero and odd harmonics will present in the signal. So the 3rd, 5th, 7th, 9th, 11th, 13th and 15th harmonics were calculated and Total Harmonics Distortion is calculated as 11.8% which is shown in Fig. 9.

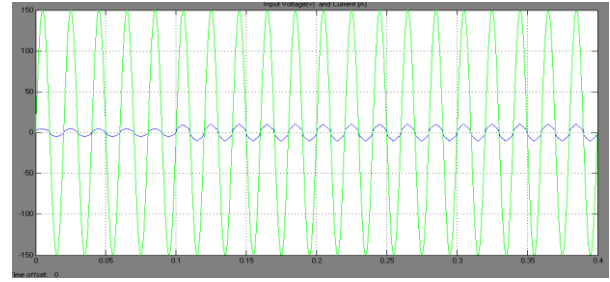


Fig. 8 V_{input} and I_{input} at 1000rpm

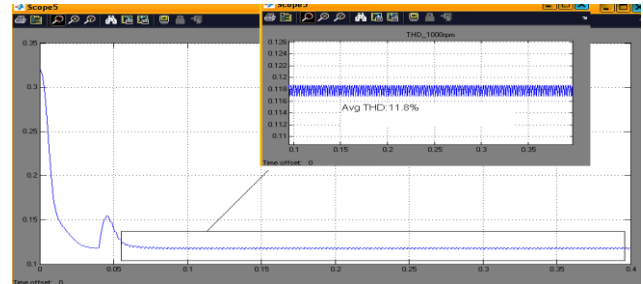


Fig. 9 THD at 1000rpm

Theoretically the frequency of machine back emf should be

$$f = (\text{speed in rpm} \times \text{no. of poles}) / 120 \text{ Hz} \quad (17)$$

For 1000 rpm speed,

$$f = (1000 \times 8 / 120) = 66.66 \text{ Hz} \quad (18)$$

The results for the BLDC back emf waveforms at 1000 rpm set speed is as shown in Fig. 10 in which the inverter is found to be operated at 66.6Hz which is obvious from theoretical calculation and three phase stator currents are shown in Fig. 11.

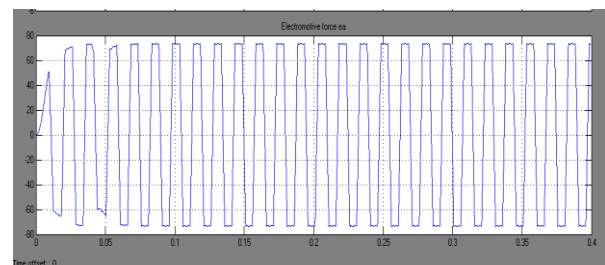


Fig. 10 Back EMF waveforms at 1000 rpm

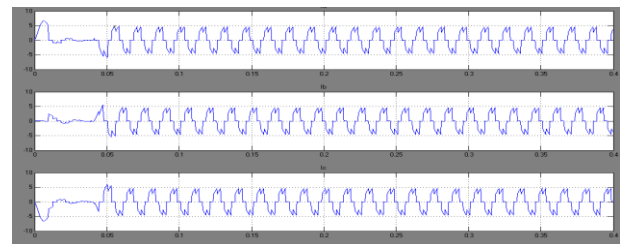


Fig. 11 Stator currents I_{abc} waveforms at 1000 rpm

The speed of the BLDC motor has set to a value of 200 rpm reference speed or set speed this time and a constant load torque of 5N.m. The corresponding speed response curve is as shown in Fig. 12.

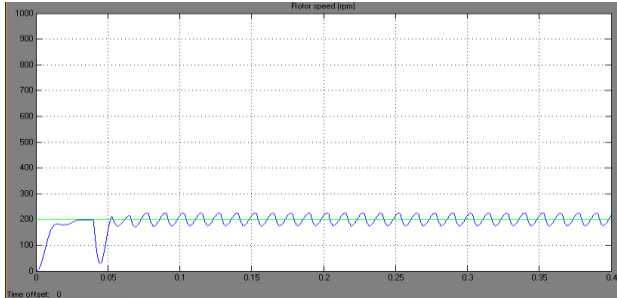


Fig. 12 Rotor Speed Curve at 200 rpm

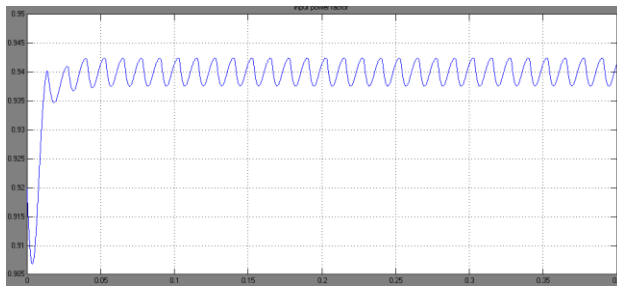


Fig. 13 Input power factor at 200 rpm

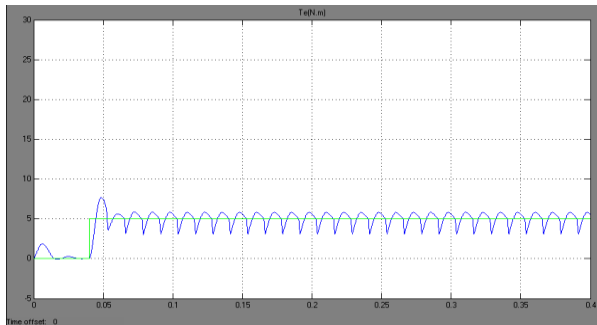


Fig. 14 Torque Curve at 200 rpm

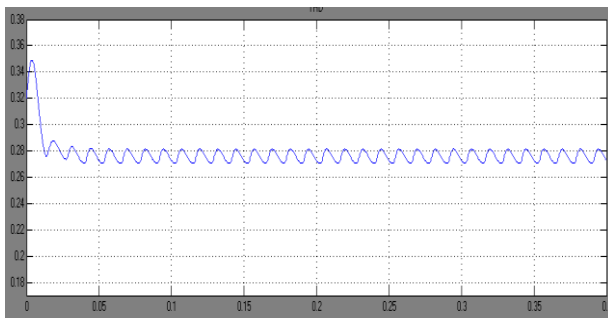


Fig. 15 THD at 200rpm

As the current is periodic waveform the even harmonic components will be zero and odd harmonics will present in the signal. So the 3rd, 5th,

7th, 9th, 11th, 13th and 15th harmonics were calculated and Total Harmonics Distortion is calculated as 27.29% as shown in fig. 15.

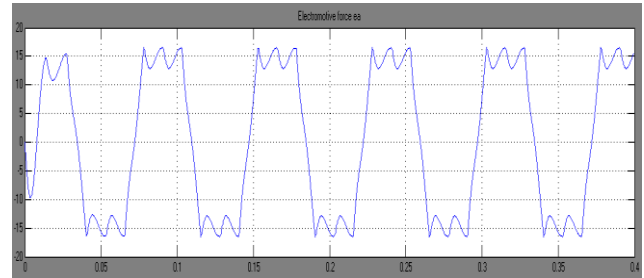


Fig. 16 Stator Back EMF waveform at 200 rpm

The results for the BLDC stator back emf waveform at 200 rpm set speed is as shown in Fig. 16 in which the inverter is found to be operated at 13.33Hz which is obvious from theoretical calculation.

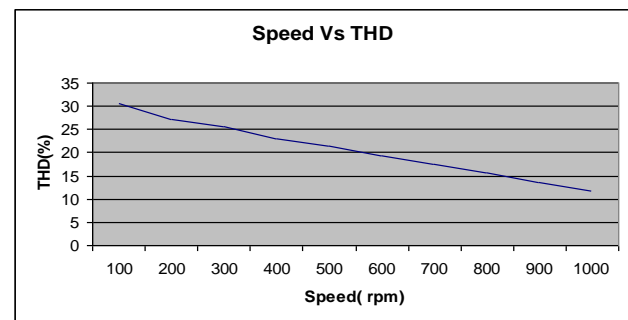


Fig. 17 Speed versus THD of input current plot

The speed versus THD of input current plot as shown in fig. 17. The total harmonic distortion for input current is high at low speed and it decreased as the set speed is increased.

Harmonic Order	200 rpm speed	700 rpm speed	1000 rpm speed
3 rd	22.62%	17.30%	7.90%
5 th	13.88%	12.51%	5.90%
7 th	3.76%	3.00%	3.40%
9 th	3.07%	2.43%	3.00%
11 th	2.6%	2.12%	2.60%
13 th	2.5%	1.88%	1.70%

Table 1. Comparison of input current harmonics as a percentage of the fundamental.

The calculated values of odd harmonics for this proposed topology for 1000 rpm, 700 rpm & 200 rpm set speeds are tabulated in Table 1. They are expressed as a percentage of the fundamental current so that the data is independent of the line voltage magnitude

The input power factor, THD and speed ripple of the drive for entire speed range 100 rpm to 1000 rpm is tabulated in Table 1. At all the speeds the power factor is improved and maintained almost unity at higher speeds. The THD and speed ripples are high at lower speeds and low at higher speeds as shown in Table 2.

Speed (rpm)	Power factor	THD (%)	Speed Ripple (%)
100	0.92	30.48	48
200	0.94	27.29	24
300	0.949	25.67	15
400	0.96	22.98	10
500	0.964	21.43	8
600	0.967	19.35	6
700	0.97	17.51	5
800	0.973	15.67	3
900	0.977	13.59	2
1000	0.98	11.87	2

Table 2. The speed, input power factor, THD and speed Ripple.

7. Conclusion

A simplified converter topology based on a SEPIC converter has been simulated for brushless dc motors to improve the power factor at supply side. The current and voltage are almost in the same phase and maintaining almost unity power factor. The input current naturally follows the input voltage to a certain extent, reducing the amount of low-order harmonics and resulting in a high power factor. It is observed that the speed ripple at higher speeds is very low and as speed is reducing the speed ripples increase.

References

1. R. Krishnan and S. Lee, "PM Brushless dc motor drive with a new power converter topology," in *Proc. IEEE IAS Annu. Meeting*, Oct. 1995, pp. 380–387.

2. R. Krishnan, "A novel single switch per phase converter topology for four-quadrant PM Brushless dc motor drive," in *Proc. IEEE IAS Annual Meeting*, vol. 1, Oct. 1996, pp. 311–318.
3. J. Skinner and T. A. Lipo, "Input current shaping in Brushless dc motor drives utilizing inverter current control," in *Proc. 5th Intl. Conf. Elect. Mach. Drives*, 1991, pp. 121–125.
4. D. S. L. Simonetti, J. Sebastián, and J. Uceda, "The discontinuous conduction mode SEPIC and Cuk power factor preregulators: analysis and design," *IEEE Trans. Ind. Electron.*, vol. 44, pp. 630–637, Oct. 1997.
5. T. Gopalarathnam, S. Waikar, H. A. Toliyat, M. S. Arefeen, and J. C. Moreira, "Development of low-cost multi-phase Brushless dc (BLDC) motors with unipolar current excitations," in *Proc. IEEE IAS Annu. Meeting*, Oct. 1999, pp. 173–179.
6. Tilak Gopalarathnam, Hamid A. Toliyat, "Input Current Shaping in BLDC Motor Drives Using a New Converter Topology" in *IECON'01: The 27th Annual Conference of the IEEE Industrial Electronics Society*, pp. 1441–1444.
7. Rahul Khopkar, S. M. Madan, Masoud HaJiaghajani, Hamid A. Toliyat, "A Low-Cost BLDC Motor Drive using Buck-Boost converter for Residential and Commercial Applications" in *IEEE conference, 2003*, pp. 1251–1257.
8. Gunhee Jang and M. G. Kim, "A Bipolar-Starting and Unipolar-Running Method to Drive a Hard Disk Drive Spindle Motor at High Speed With Large Starting Torque" in *IEEE Transactions on Magnetics*, Vol. 41, No. 2, February 2005, pp. 750–755.
9. Chee-Mun Ong, "Dynamic Simulation of Electric Machinery using Matlab/Simulink", 1998.
10. Paul C. Krause, Oleg Wasynczuk and Scott D. Sudhoff, "Analysis of Electric Machinery & Drive Systems", 2nd Edition, IEEE Press, Wiley InterScience.
11. W. Shepherd, L. N. Hulley and D. T. W. Liang, "Power Electronics and Motor Control", 2nd Edition, Cambridge University Press, 2005.
12. Gunhee Jang and M. G. Kim, "A Bipolar-Starting and Unipolar-Running Method to Drive a Hard Disk Drive Spindle Motor at High Speed With Large Starting Torque" *IEEE Transactions on Magnetics*, Vol. 41, No. 2, February 2005.
13. Chee-Mun Ong, *Dynamic Simulation of Electric Machinery using MATLAB/Simulink*, 1998.